Target poisoning during CrN deposition by mixed high power impulse magnetron sputtering and unbalanced magnetron sputtering technique

PURANDARE, Yashodhan <http://orcid.org/0000-0002-7544-9027>, EHIASARIAN, Arutiun <http://orcid.org/0000-0001-6080-3946> and HOVSEPIAN, Papken <http://orcid.org/0000-0002-1047-0407>

Published version

PURANDARE, Yashodhan, EHIASARIAN, Arutiun and HOVSEPIAN, Papken (2016). Target poisoning during CrN deposition by mixed high power impulse magnetron sputtering and unbalanced magnetron sputtering technique. Journal of Vacuum Science & Technology A, 34 (4), 041502-1.

Copyright and re-use policy

JVSTA Journal of Vacuum Science & Technology A

Target poisoning during CrN deposition by mixed high power impulse magnetron sputtering and unbalanced magnetron sputtering technique

Yashodhan P. Purandare, Arutiun P. Ehiasarian, and Papken Eh Hovsepian

Citation: Journal of Vacuum Science & Technology A **34**, 041502 (2016); doi: 10.1116/1.4950886
View online: http://dx.doi.org/10.1116/1.4950886
View Table of Contents: http://scitation.aip.org/content/avs/journal/jvsta/34/4?ver=pdfcov
Published by the AVS: Science & Technology of Materials, Interfaces, and Processing

Target poisoning during CrN deposition by mixed high power impulse magnetron sputtering and unbalanced magnetron sputtering technique

Yashodhan P. Purandare,[a] Arutiun P. Ehiasarian, and Papken Eh Hovsepian
National HIPIMS Technology Centre, Materials, and Engineering Research Institute, Sheffield Hallam University, Sheffield S1 1WB, United Kingdom

(Received 23 February 2016; accepted 6 May 2016; published 18 May 2016)

Target poisoning phenomenon in reactive sputtering is well-known and has been studied in depth over the years. There is a clear agreement that this effect has a strong link on the quality, composition, properties, and pronouncedly on the deposition rate of physical vapor deposition coatings. With the introduction of ionized physical vapor deposition techniques such as the relatively novel high power impulse magnetron sputtering (HIPIMS), which have highly ionized plasmas of the depositing species (metal and gas ions), target poisoning phenomenon is highly contested and thus has been left wide open for discussion. Particularly, there have been contradicting reports on the presence of prominent hysteresis curves for reactive sputtering by HIPIMS. More work is needed to understand it, which in turn will enable reader to simplify the coating deposition utilizing HIPIMS. This work focuses on the study of chromium (Cr) targets when operated reactively in argon + nitrogen atmosphere and in different ionizing conditions, namely, (1) pure HIPIMS, (2) HIPIMS combined with unbalanced magnetron sputtering (UBM), and (3) pure UBM. Nitrogen flow rate was varied (5–300 sccm) whereas the average power on target was maintained around 8 kW. Target resistance versus N_2 flow rate curves for these conditions have been plotted in order to analyze the poisoning effect. When only one UBM target was operating target poisoning effect was prominent between the flow rates of 80 and 170 sccm. However, it appeared reduced and in nearly same flow rate ranges (90 and 186 sccm) when only one HIPIMS target was operating. When four UBM targets were operated, target poisoning effect was evident, however, expectedly moved to higher flow rates (175 sccm and above) whereas appeared diminished when two UBM and two HIPIMS were running simultaneously. Further, to analyze the effect of actual target conditions (poisoning) on deposition rate and on the properties of the films deposited, commercially widely used chromium nitride (CrN) coatings were deposited in mixed HIPIMS and UBM plasma and at five different flow rates of nitrogen. Detail characterization results of these coatings have been presented in the paper which will assist the reader in deposition parameter selection. [http://dx.doi.org/10.1116/1.4950886]

I. INTRODUCTION

Over the years, reactive sputtering has been thoroughly investigated and reported by various researchers. It is well known that in reactive sputtering, the formation of a compound layer on the target alters the voltage–current characteristics of the target and is termed as target poisoning. This can have a detrimental effect on the sputtering process stability, on the coating deposition rate, and microstructure leading to an effect on the properties of the coatings deposited. Target poisoning phenomenon has shown a complex but sensitive relation to the target powers and reactive gas partial pressures, which in turn are related to the energetic ions/neutrals in the vicinity of the target surface.[1]

In high power impulse magnetron sputtering (HIPIMS) and in most ionized physical vapor deposition processes (IPVD), due to high target powers (in a pulse) and highly ionized flux (reactive and process gases and metal species) in the vicinity of the target and in the deposition chamber space,[2] the situation is more complex. It was reported that in highly ionized plasmas, poisoning mechanism can include both chemisorption and reactive ion implantation.[3,4] However, there have been contradicting reports on the hysteresis of HIPIMS technique and it needs further work to understand this complex phenomenon in this relatively novel technique. Various authors have reported a clear hysteresis for HIPIMS (Refs. 4–6) whereas some of the literature suggests that hysteresis can be suppressed/reduced by controlling the process/power supply parameters[7–11] or can be completely absent.[12]

Current work focuses on target poisoning studies on a chromium (Cr) target in a combined argon and nitrogen atmosphere when operated in HIPIMS and will add to the knowledge base of target poisoning phenomenon in HIPIMS. It has been shown that HIPIMS itself can be used as a coating deposition technology[13] or as a tool (in combination with other techniques) to ionize plasma which otherwise is depleted of energetic flux, e.g., DC sputtering.[14] For example, when combined with DC-unbalanced magnetron sputtering (referred henceforth as UBM), HIPIMS can address some of the issues of deposition rates and can give a greater control over the properties of magnetron sputtered coatings.[15,16] Eventually combining HIPIMS with UBM further makes things complex but interesting from target poisoning point of view. Thus, this work also investigates the

[a]Author to whom correspondence should be addressed; electronic mail: Y.Purandare@shu.ac.uk

poisoning effects of a chromium (Cr) target when operated in HIPIMS mode but in a combination of HIPIMS + UBM technology in an $Ar + N_2$ reactive environment. Based on the results of these poisoning studies, five different sets of CrN coatings, widely preferred in the industry, were synthesized using the combined HIPIMS + UBM technology. The flow rates chosen for these individual depositions represent broadly the flow range used for investigating poisoning effect. Detail characterization of these coatings (microstructural and mechanical properties) has been done to understand the actual effect of target conditions on the properties of the coatings in these conditions. The results provide a new aspect to job coaters in the form of a combined HIPIMS + UBM technology to expand their horizon as the results can also be implied on other coating combinations.

II. EXPERIMENT

This work was carried out in an industrial sized PVD machine (1000-4 HTC, Hauzer techno coatings, Netherlands). The machine has a chamber size of 1 m^3 with four rectangular planer targets (sized 600 × 200 mm) which can be operated in UBM or HIPIMS mode. The machine is fitted with HIPIMS power supplies from Hüttinger Electronic Sp. z o.o., Poland. These generators can supply power pulses with duration in the range of 0–200 μs at a frequency of 0–500 Hz (2 ms) equivalent to a duty cycle of 10%. Peak currents of up to 3000 A and at a voltage of 2000 V can be achieved.

In the current set of experiments, target poisoning studies were performed on Cr targets. Target resistance of one Cr target was calculated when that target was operated (and other three targets) in the following conditions: (1) HIPIMS + other three off; (2) UBM + other three off; (3) two HIPIMS + two UBM simultaneously; and (4) four UBM simultaneously. Figure 1 shows the schematic representation of the deposition chamber along with the target arrangement.

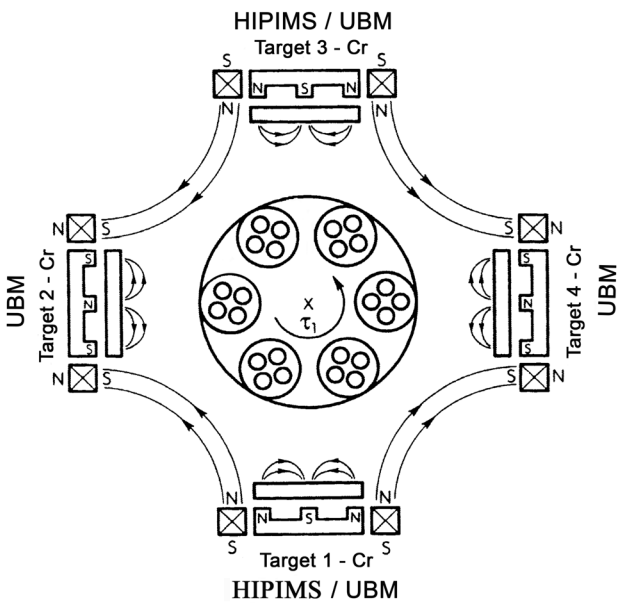

FIG. 1. Schematic representation of the Hauzer-1000 four target deposition system with the operation mode.

The machine was operated in the constant power mode where the average power on the target(s) was always maintained at 8 kW irrespective of the technology (UBM/HIPIMS) and study conditions described above. When HIPIMS was utilized, the generators were used in a nonsynchronized mode with 200 μs long pulses at a frequency of 100 Hz, both which were held constant along with the peak voltage.

During the measurements, Ar was used as the sputtering gas with a constant flow of 200 sccm. Precise control of N_2 flow was achieved with the help of a reactive gas controller system (SPEEDFLO V6, Gencoa, Ltd.) where the gas flow was systematically ramped from 5 to 300 sccm over a time interval of 20 min (ramping rate of approximately 0.25 sccm per second) and then reduced at the same rate. Average values of target current and voltage during pure DC (UBM) operation whereas peak pulse current and voltage values in the case of HIPIMS were recorded every 20 s for the target resistance calculations. Pumping speed was held constant for all experiments irrespective whether one or four targets were in operation.

It is well known that HIPIMS plasmas are rich in metal and gas ions which can be effectively utilized to pretreat the surfaces before deposition to improve adhesion[17] or deposit dense coatings. It is also understood that HIPIMS can also be treated as an IPVD technology without the necessity of any external ionization devices, as the metal flux being deposited is ionized along with the reactive and process gases. Thus, it can be combined with other techniques such as UBM to reap the benefits of enhanced ionization, but with greater flexibility over deposition conditions such as bias voltage, deposition temperature, as well as acceptable deposition rate.[15,16,18]

Based on the poisoning study results, five different sets of CrN coatings were deposited with the combined HIPIMS and UBM technology. Five different flow rates of reactive gas (N_2), namely: (1) 75, (2) 110, (3) 150, (4) 200, and (5) 250 sccm were chosen representing the broad flow range utilized in the target poisoning studies presented above. Coatings were deposited in a combined $Ar + N_2$ atmosphere (Ar flow rate was held constant at 200 sccm) at a deposition temperature of 400 °C and with a bias voltage of Ub = − 65 V in threefold rotation. Average power on the target was maintained at 8 kW irrespective of the technology used and each deposition run lasted 90 min. As stated above, apart from N_2 flow rate, all other parameters were maintained constant. Prior to coating deposition, substrates were pretreated with Cr^+ ions generated with HIPIMS plasma to improve adhesion.[17]

Coatings were deposited on a polished 1 μm finish high speed steel (HSS), 316L stainless steel, and Si (001) wafers which were used for characterization. The coatings were characterized in terms of their structural, mechanical, and tribological properties with a number of analytical techniques. These include scratch adhesion test (ANTON PAAR-CSM REVETEST) for determination of critical load (L_{C2} according to BS EN 1071-3 standard) and nanohardness tests to measure hardness (CSM nanoindenter). The sliding wear coefficients (ANTON PAAR-CSM TRIBOMETER) were calculated by subjecting the specimens at a linear velocity of 0.1 ms^{-1} sliding against a 6 mm Al_2O_3 ball for a distance of

3769 m (60 000 laps) under normal load of 5 N. Sliding wear rates were calculated by measuring volume loss in a wear track with a stylus profilometer (DEKTAK 150) having a lateral resolution of 33 nm. Glancing angle x-ray diffraction technique was used for structural phase and stress analysis [PANalytical Empyrean]. Coating thickness and microstructure analysis was conducted by cross-sectional microscopy using a scanning electron microscope (NOVA-NanoSEM). Details of the deposition chamber, characterization techniques, and analytical instruments can be found in a previous publication.[14]

III. RESULTS AND DISCUSSION

A. Target resistance curves

As stated in the experimental section, four sets of target operation conditions were studied. While employing the UBM technology, DC generators were operated in constant power mode (changing voltage); while for HIPIMS the generators were used in constant voltage mode (changing peak current and power). These respective modes of operation of the power supplies produced the most stable discharge conditions and hence were used in the current set of experiments. In order to compare hysteresis effect from these two different technologies and operation mode, it was important to find a normalization factor. Thus, electrical resistance of the target as an effect of changing target condition (poisoning with changing N_2 flow) was calculated and compared. Figures 2–5 show the changing target resistance and total gas pressure of the chamber as an effect of changing N_2 flow and deposition technology.

1. One target HIPIMS

Figure 2 shows the changing resistance and total gas pressure of the Cr target with changing N_2 flow when only one target was operated in HIPIMS mode. As visible in this figure, the total gas pressure increased and decreased linearly with the gas flow for the flow range studied. Between flow rates of 5 and 100 sccm, target resistance remains at near similar values; around 3 Ω. It is now well known that the

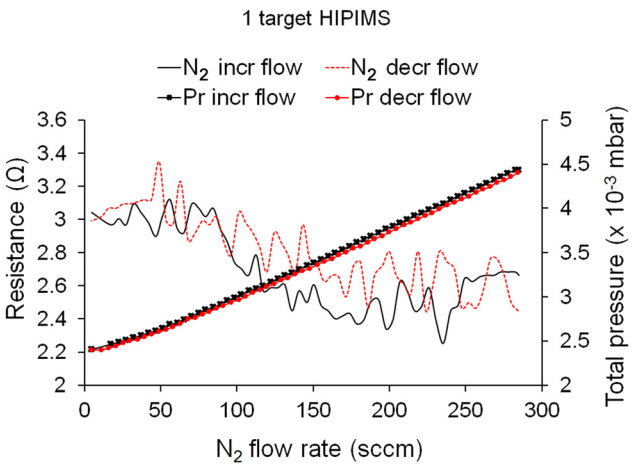

FIG. 2. (Color online) Target resistance and total gas pressure vs N_2 flow rate curves: one target in the HIPIMS mode.

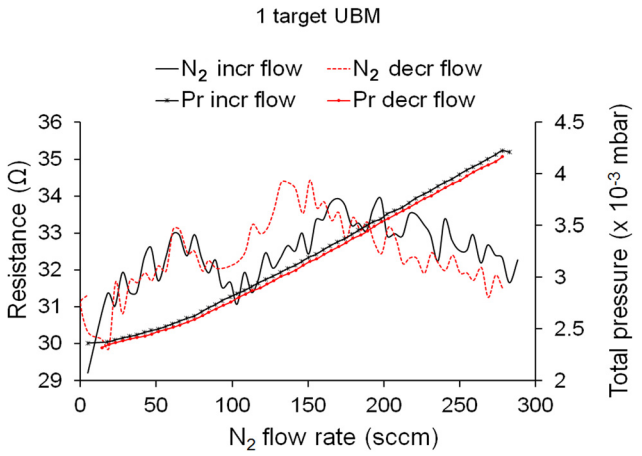

FIG. 3. (Color online) Target resistance and total gas pressure vs N_2 flow rate curves: one target in the UBM mode.

dissociation and ionization of reactive gases in HIPIMS plasma is equally effective as that of the target material[18] and can lead to enhanced chemical reactions. Thus, any N_2 gas admitted to the chamber in this flow range (5–100 sccm) will readily react and get consumed at substrate surfaces and/or chamber walls without substantially affecting the target much;[19] also evident from the total gas pressure measurements in this case (Fig. 2). For flow rates between 100 and 200 sccm target resistance drops at a faster rate (drop from 3 to 2.4 Ω). This phase, which also corresponded to the increase in pulse peak current measured, could be attributed to the rise in ionic currents resulting from increased ionization of the flux (gas + metal) resulting from enhanced collisions with the energetic electrons in the discharge.[6] On further increase in the N_2 flow rate, beyond 200 sccm, target resistance shows an increase in values around 2.8 Ω. Since the electrical conductivity of CrN has been found to be dependent on its stoichiometry,[20] this complex behavior of changing resistivity of the target can be attributed to the changes in thickness, distribution, and changing stoichiometry of the compound formed on the target surface. On the

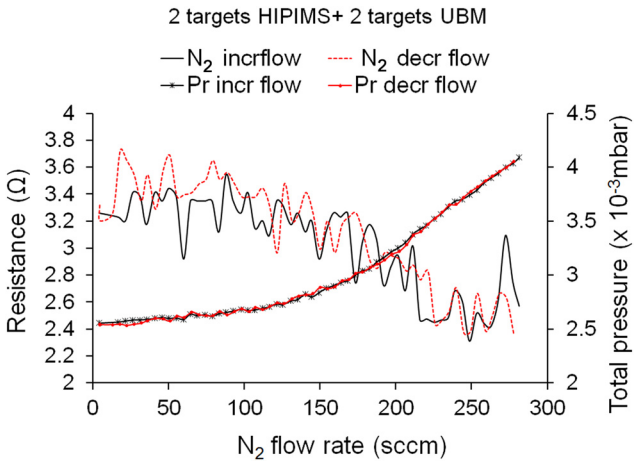

FIG. 4. (Color online) Resistance of a HIPIMS cathode and total gas pressure vs N_2 flow rate curves: two targets in the HIPIMS mode and two targets in the UBM mode.

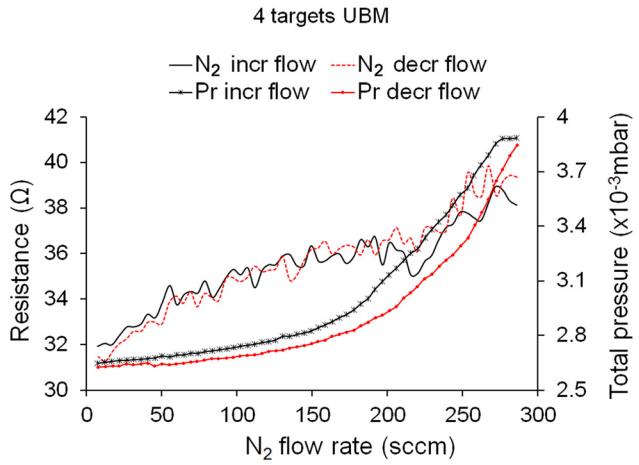

FIG. 5. (Color online) Resistance of a UBM cathode and total gas pressure vs N_2 flow rate curves: all targets in the UBM mode.

reverse sweep of flow rates, the poisoning hysteresis, though weak, is visible between flow rates around 100–200 sccm.

2. One target UBM (DC)

Figure 3 shows the target resistance and total gas pressure versus N_2 flow curves when the target is operated in UBM mode. It can be observed that target resistance increases almost linearly with N_2 flow rate until almost 75 sccm. Also the slope of the total gas pressure curve is less steep in this flow range. The results suggest that any N_2 gas added to the chamber is readily consumed at the target and contributes to its poisoning. Thus, the decrease in target current measured (increasing voltage for a DC generator in constant power mode) is a direct result of continuously reducing sputtering yield owing to the formation of a compound which has a higher secondary electron emission yield.[19] At this stage (75 sccm), it could be estimated that the target is thoroughly covered by the nitride and any addition of reactive gas would lead to its stoichiometric changes and/or its thickening. On further increase in the reactive gas flow in the chamber, target resistance slightly dropped (around flow rates 75–100 sccm), however, picked up again until flow reached around 170 sccm. Beyond 170 sccm, the resistance showed a continuous drop again. Target poisoning is governed by the equilibrium between the gas flow and three drains for the reactive gas: (1) the pumping speed, (2) reaction with deposited substrate /walls, and (3) reaction on the target. Since the pumping speed was kept constant in all the cases, the deposition rate of material on the chamber walls and the buildup of compound on the target are inversely related. Thus, the complex behavior of changing resistance of the target can be attributed mainly to the changes in stoichiometry of the compound and its thickness formed on the surface of the target. The poisoning hysteresis is prominent as compared to pure HIPIMS and clearly visible in between flow rates of 70 and 170 sccm. Comparing results from Figs. 2 and 3 and the fact that decrease in resistance with almost linearly rising gas total pressure, Fig. 2, suggests that the formation of compound at the target surface and its removal by sputtering is much more dynamic in the case of HIPIMS as compared to UBM sputtering processes (Fig. 3).

3. Two targets HIPIMS and two targets UBM (DC)

Figure 4 shows the target resistance and total gas pressure recorded when the target was operated in the HIPIMS mode along with one more target in HIPIMS and two targets in UBM mode simultaneously. As observed for the conditions of one target in HIPIMS, target resistance showed no significant change until the N_2 flow rates reached 100 sccm. From flow rates of 100 to until 270 sccm, resistance continuously dropped, apart from the sharp increase in between flow rates of 275–300 sccm. Total gas pressure curves show no hysteresis effect and follow closely with the ramping. However, it shows two distinct phases: (1) almost steady and flat slope below 130 sccm flow range and (2) almost linearly increasing beyond 130 sccm. This suggests that target poisoning in this case is initiated at much lower flow ranges of N_2 as compared to the flow range of around 100–200 sccm observed for the case of one target HIPIMS, Fig. 2 as well as around flow range of 70–170 sccm as observed in the case of one UBM (Fig. 3). Like for pure HIPIMS (one target in HIPIMS mode and others off), target compound formation and its removal is more dynamic.

4. Four targets UBM (DC)

Figure 5 shows the results for the target resistance and total gas pressure when operated in pure UBM mode along with all the rest of the targets also in the UBM mode. Resistance showed a continuous upward trend until flow rates reached around 300 sccm, with the exception of a small drop between N_2 flow rates between 200 and 250 sccm. The target poisons almost readily when nitrogen is admitted to the chamber, evident from the gas pressure graphs, and is much more severe compared to the situation where HIPIMS is combined with UBM. During the initial coverage of the target surface with a compound layer, the total pressure rises slowly and the resistance increases monotonically. Due to increased surface area (now four targets acting as drains), this process continues up to a gas flow of around 200 sccm. The same behavior of target resistance and total chamber pressure is also seen in the case of single target operating in UBM mode, Fig. 3; however, due to only one target acting as a drain, it occurs at lower flow rates of nitrogen of around 75 sccm.

B. Coating deposition

Figures 6(a)–6(e) show the SEM cross-sectional micrographs of the coatings produced on Si substrate with different N_2 flow rates, namely: (a) 75 sccm, (b) 110 sccm, (c) 150 sccm, (d) 200 sccm, and (e) 250 sccm. It can be clearly seen that in all the cases coatings with very dense columnar grains were deposited. The columnar grains have a diameter of around 300–350 nm which terminate into a dome-shaped structure typical of DC sputtered coatings. However, as a result of intentional low energy ion-bombardment during their growth, they appeared to be very densely packed to the extent that it was difficult to resolve the grain boundaries.

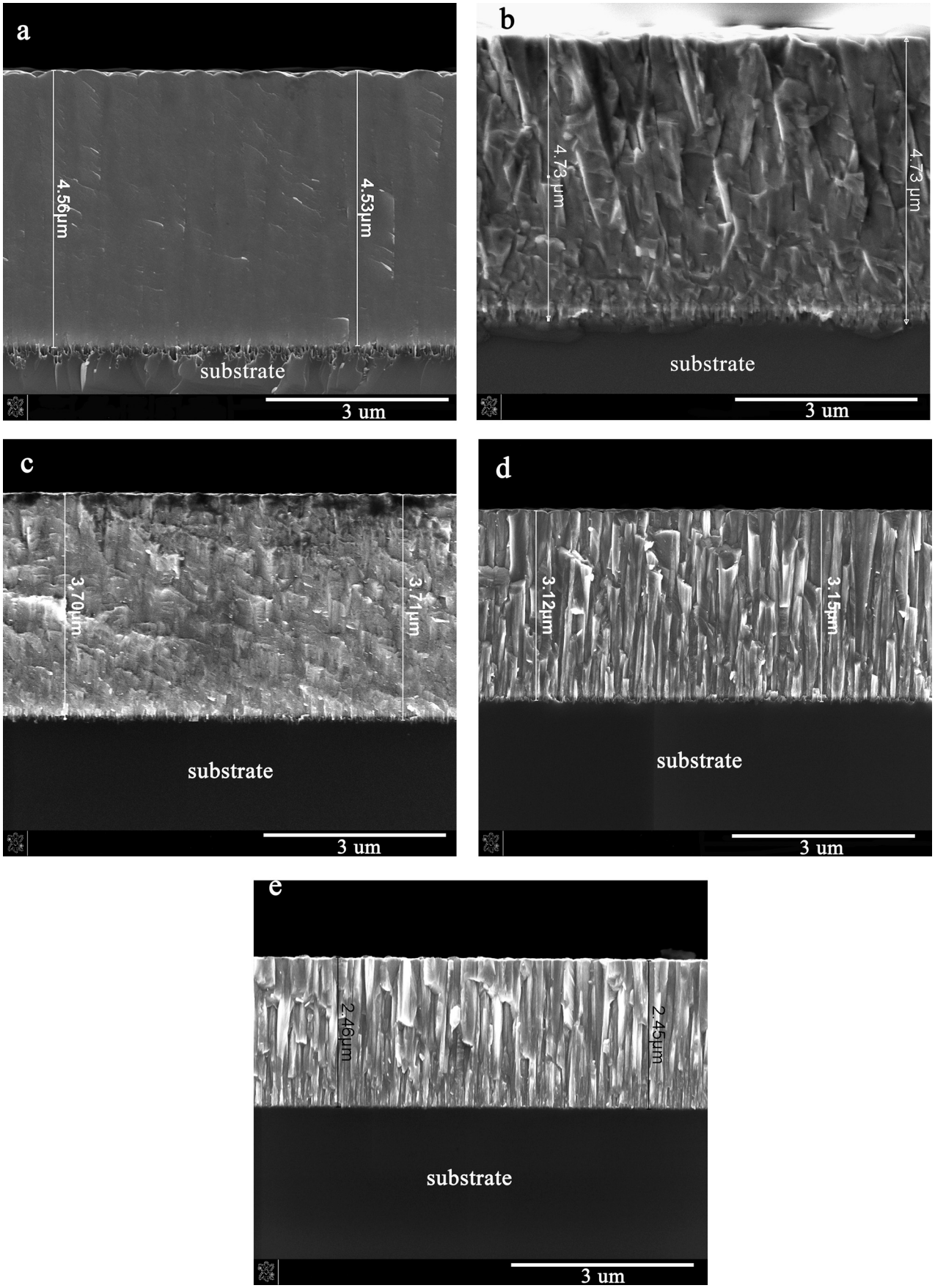

FIG. 6. SEM cross-sectional images of coatings with different N_2 flow rates: (a) 75 sccm, (b) 110 sccm, (c) 150 sccm, (d) 200 sccm, and (e) 250 sccm.

TABLE I. Stoichiometry and thickness results obtained by cross-sectional SEM studies.

N_2 flow rate	Total gas pressure ($\times 10^{-3}$ mbar)	Composition (at. %) (Cr:N)	Thickness (μm)	Deposition rate (nm m^{-1})
75	2.60	77.2:22.8	4.54	50.4
110	2.68	68.5:31.5	4.73	52.5
150	2.87	53.6:46.4	3.70	41.1
200	3.33	47.7:52.3	3.13	34.7
250	3.88	45.9:54.1	2.45	27.2

The dome shape appeared very prominent for the lowest N_2 flow rate condition; however, it diminished as the flow rate increased resulting into flatter surfaces. The cross-section appeared glassy for lowest N_2 flow rate, Fig. 6(a), and became faceted [Figs. 6(b)–6(e)] as the flow rate increased. Similar dependency of microstructure on nitrogen flow rate of CrNx coatings has been reported by Greczynski *et al.* when pure HIPIMS along with a high pulsed bias voltage of −150 V was used.[21] However, the authors report that, for the same pulse energy, above a critical nitrogen content in the films (33 at. %), transition from a column free, nanosized grain structure into more obvious columnar grain structure takes place. Thus, in the current set of results, the columnar structure observed for all the coatings, irrespective to the nitrogen content in the film, can be largely accounted to the UBM flux. As clearly evident from the images, the deposition rate changed significantly as the N_2 flow rate increased. With increasing N_2 flow rates (increase in nitrogen partial pressure), more of the deposition flux will undergo diffusive collisions and can be accounted for this drop in deposition rate along with the phenomenon of redeposition and target poisoning. The coating composition and thickness data (thus deposition rate) has been compiled and summarized in Table I. As evident from the EDX results, coatings with N_2 flow rate of 150 and 200 sccm had near stoichiometric composition.

Figure 7 shows the results of coating phase analysis using glancing angle XRD technique. The results indicate that in the case of coatings with low nitrogen flow rates; typically at 75 sccm, the texture was dominated by hexagonal closed packed (hcp) Cr_2N (200) peaks with a weaker presence of other orientations such as (002), (111), (112), (211), and (200). The presence of face center cubic (fcc) CrN (111) intertwined with Cr_2N (200) peaks suggested that coating had a mixed $Cr_2N + CrN$ crystalline structure. As the nitrogen flow increased to 110 sccm, fcc CrN (200), (111), (311) peaks started appearing at the expense of Cr_2N peaks. Cr_2N peaks completely disappeared when the flow rate was increased to 150 sccm and the coating structure appeared with fcc CrN crystals. Further increasing the N_2 gas proportion, peaks from fcc CrN become prominent.

These coatings were extensively characterized to analyze the effect of N_2 flow rate on the coating properties (deposited on HSS substrate). Table II shows these results obtained in detail. The beneficial effect of HIPIMS etching and HIPIMS assisted superior dense defect free microstructure (free of voids, macrosized growth defects) can be seen on the properties of these coatings. All the coatings analyzed have a scratch adhesion value of $L_{C2} > 80$ N. The coatings had a high hardness values in the range of 22–30 GPa depending on the flow rate. These coatings also had a very high dry sliding wear resistance (in the range of 10^{-16}) with the exception of coating b (N_2 flow rate = 110 sccm) which had a slightly lower wear resistance and highest friction coefficient ($\mu = 0.59$) among the coatings tested. It can be attributed to its low hardness

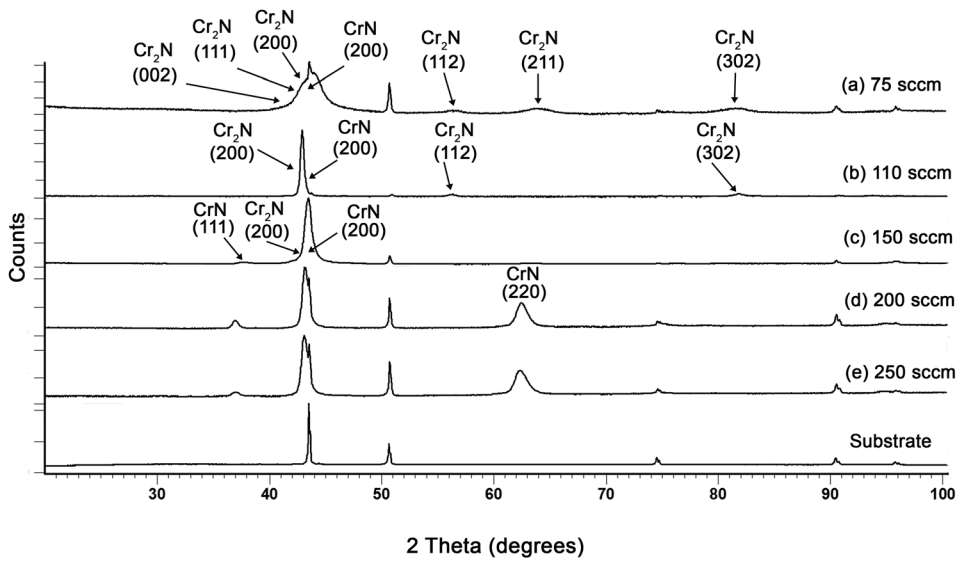

FIG. 7. Coating phase analysis: x-ray diffractograms recorded for coatings with different N_2 flow rates: (a) 75 sccm, (b) 110 sccm, (c) 150 sccm, (d) 200 sccm, and (e) 250 sccm.

TABLE II. Characterization results obtained from various tests carried out on the coatings.

Coating reference	Nanohardness (GPa)	Young's modulus (GPa)	Stress (GPa)	Ra (μm)	Wear coefficient, K_C ($m^3\ N^{-1}\ m^{-1}$)	Friction coefficient (μ)
a	25 ± 1.8	394 ± 60	—	0.048	6.54×10^{-16}	0.47
b	21 ± 2.8	398 ± 88	—	0.050	4.89×10^{-15}	0.59
c	26 ± 3.3	373 ± 41	-2.5 ± 0.18	0.054	1.48×10^{-16}	0.43
d	31 ± 1.7	453 ± 38	-4.6 ± 0.27	0.047	1.98×10^{-16}	0.40
e	31 ± 3.1	411 ± 59	-1.9 ± 0.12	0.043	2.91×10^{-16}	0.36

(21 GPa) as compared to other coatings. Calculations revealed that the coatings had compressive residual stresses in the range of 1.9–4.6 depending on the flow rates. In the case of coatings a and b (75 and 110 sccm flow rates), it was difficult to calculate stress values as the Cr_2N and CrN peaks were overlapping and hence have not been reported. All the coatings had a near similar roughness values in the range of 0.04–0.05, which can be attributed to the dense microstructure irrespective of its stoichiometry. In general, all the coatings have a high dry sliding wear resistance and high adhesion values, independent of the nitrogen flow rate used. It is notable especially when the coating thickness is different.

IV. SUMMARY AND CONCLUSIONS

Cr target poisoning studies in a reactive atmosphere (nitrogen + argon) were successfully conducted in an industrial sized deposition chamber operated by different technologies, namely, pure HIPIMS, pure UBM, and combined HIPIMS + UBM techniques. Also, CrN deposition was successfully carried out at faster deposition rates by combining HIPIMS and UBM technologies. Very dense coatings were produced even at low nitrogen flow rates. This is a significant achievement since low bias voltages were used and literature suggests that DC or magnetron sputtered coatings often have less dense or porous structures when lower nitrogen flow rates are used. The following can be concluded from the current set of experiments employed:

(1) As anticipated, target poisoning was prominent when targets were operated in UBM technique. The hysteresis was observed in the N_2 flow range of 70 and 170 sccm when one target was operational; however, it was pushed to higher flow rates of 200 sccm and above when all four targets were operating in UBM mode.
(2) When run in pure HIPIMS or in combination with UBM, in general, the target resistance decreased with increasing nitrogen flow rate; poisoning hysteresis appeared to be narrowed. Compound formation and removal at the target surface was more dynamic as compared to DC-UBM.
(3) The phase composition of the coatings deposited by HIPIMS + UBM technique changed from mixed Cr_2N + CrN to fcc CrN dominated when the flow rate of nitrogen was increased to 150 sccm, and with preferred (111) orientation when the flow rate was 200 and 250 sccm.
(4) In general, irrespective of the nitrogen flow rates, CrN coatings deposited in this study appeared to have very dense, defect free columnar microstructure (no intercolumnar voids), which when combined with high adhesion leads to high hardness and wear resistance.

[1]W. D. Sproul, P. J. Rudnik, and C. A. Gogol, Thin Solid Films **171**, 171 (1989).
[2]A. P. Ehiasarian, R. New, W.-D. Münz, L. Hultman, U. Helmersson, and V. Kouznetsov, Vacuum **65**, 147 (2002).
[3]D. Depla and R. De Gryse, Surf. Coat. Technol. **183**, 184 (2004).
[4]M. Audronis and V. Bellido-Gonzalez, Thin Solid Films **518**, 1962 (2010).
[5]M. Audronis, V. Bellido-Gonzalez, and B. Daniel, Surf. Coat. Technol. **204**, 2159 (2010).
[6]C. Nouvellon *et al*., Surf. Coat. Technol. **206**, 3542 (2012).
[7]E. Wallin and U. Helmersson, Thin Solid Films **516**, 6398 (2008).
[8]K. Sarakinos, J. Alami, C. Klever, and M. Wuttig, Surf. Coat. Technol. **202**, 5033 (2008).
[9]T. Kubart, M. Aiempanakit, J. Andersson, T. Nyberg, S. Berg, and U. Helmersson, Surf. Coat. Technol. **205**, S303 (2011).
[10]A. Surpi, T. Kubart, D. Giordani, M. Tosello, G. Mattei, M. Colasuonno, and A. Patelli, Surf. Coat. Technol. **235**, 714 (2013).
[11]M. Aiempanakit, T. Kubart, P. Larsson, K. Sarakinos, J. Jensen, and U. Helmersson, Thin Solid Films **519**, 7779 (2011).
[12]D. Benzeggouta, M. C. Hugon, and J. Bretagne, Plasma Sources Sci. Technol. **18**, 045026 (2009).
[13]A. Ehiasarian, W. D. Münz, L. Hultman, U. Helmersson, I. Petrov, and F. Seitz, Galvanotechnik **94**, 1480 (2003).
[14]Y. P. Purandare, A. P. Ehiasarian, and P. Eh. Hovsepian, J. Vac. Sci. Technol., A **26**, 288 (2008).
[15]P. Eh. Hovsepian, A. A. Sugumaran, Y. Purandare, D. A. L. Loch, and A. P. Ehiasarian, Thin Solid Films **562**, 132 (2014).
[16]J. Paulitsch, M. Schenkel, Th. Zufraß, P. H. Mayrhofer, and W.-D. Münz, Thin Solid Films **518**, 5558 (2010).
[17]A. P. Ehiasarian, J. G. Wen, and I. Petrov, J. Appl. Phys. **101**, 054301 (2007).
[18]A. P. Ehiasarian, Y. Aranda Gonzalvo, and T. D. Whitmore, Plasma Processes Polym. **4**, S309 (2007).
[19]G. Bertrand, C. Savall, and C. Meunier, Surf. Coat. Technol. **96**, 323 (1997).
[20]E. Martinez, R. Sanjinés, O. Banakh, and F. Lévy, Thin Solid Films **447–448**, 332 (2004).
[21]G. Greczynski, J. Jensen, J. Böhlmark, and L. Hultman, Surf. Coat. Technol. **205**, 118 (2010).